A Lean Control Theoretic Approach to Energy-Harvesting in Diffusion-Based Molecular Communications

Vittoria Musa, *Student Member, IEEE,* Giuseppe Piro, *Member, IEEE,* Luigi Alfredo Grieco, *Senior Member, IEEE,* and Gennaro Boggia, *Senior Member, IEEE*

***Abstract*—This letter focuses on a diffusion-based molecular communication system, fed by a nanoscale energy-harvesting mechanism, and conceives a power control mechanism based on feedback control theory. Specifically, the load current drained by the transmitter interface is set proportionally to the available energy harvested from the environment by using a closed-loop control scheme. The resulting system is analytically described through a nonlinear state equation, that jointly considers harvesting and discharging processes. Its asymptotic stability is evaluated around the equilibrium point, while considering some technological constraints. Finally, a numerical example is discussed to clearly show the behavior of the proposed approach in conceivable scenarios.**

***Index Terms*—Diffusion-based Molecular Communication; Energy-Harvesting; System Model; Control Theory.**

I. Introduction

The diffusion-based molecular communication is a key enabling technology for the Internet of Bio-Nano Things: it allows to disseminate information molecules between nano-devices, even in scenarios where a dedicated biological infrastructure does not exist (molecules can reach destination devices by diffusion, while ensuring transmission ranges up to tens micrometers) [1]–[3]. The generation, release, and reception of molecules (i.e., hormones, pheromones, proteins, DNA, and RNA) cause a non-negligible amount of energy consumption [4], [5]. Thus, considering that nano-devices can use a limited energy budget available within battery with restricted capabilities [2], it is of paramount importance to conceive advanced techniques offering long-lasting communication capabilities at both nano and microscales [6].

The scientific literature on harvesting-communication systems at the macroscale is significantly large and embraces many methodologies applicable to heterogeneous communication technologies and application domains [7], [8]. However, traditional approaches (e.g., those leveraging solar, wind, and thermal energy) seem to be inefficient at nano and microscales. Here, it is preferable to use different energy harvesting models, based on mechanical and chemical sources [9], [10]. Recent advancements in the nanotechnology field offer the opportunity to harvest the energy from external vibrations (e.g., the human heartbeat in in-vivo applications) through piezoelectric nanogenerators made up by Zinc Oxide nanowires [11], [12]. Some contributions already envisaged to adopt piezoelectric nanogenerators to feed nano-devices willing to communicate through electromagnetic waves in the Terahertz band [13] or to selectively stimulate peripheral nerves in the human body through light signals [14], [15].

With reference to diffusion-based molecular communications, some works formulated interesting energy-aware communication mechanisms. The molecule harvesting concept, according to which the energy cost due to the generation of molecules can be reduced by retrieving chemical material from the surrounding environment, is presented in [16], [17]. Here, a further energy saving can be achieved by exploiting relay nodes [5], [18]. Unfortunately, none of the works presented in [5], [16]–[18] considers all the energy needs related to the communication process and the actual energy budget available within nano-devices, as explicitly highlighted in [18]. Moreover, to the best of authors' knowledge and according to a recent survey on molecular communication [6], the joint integration of energy-harvesting mechanisms that leverage piezoelectric nanogenerators and energy-aware transmission scheme for diffusion-based molecular communications still remains an unexplored research topic.

Hereby, to bridge this gap, a feedback control approach is proposed. Specifically: 1) by inheriting from the work in [13], the harvesting process has been modeled as an ideal voltage source in series with a resistor and a ultra-nanocapacitor; 2) the discharging process has been modeled through a current generator in parallel with the aforementioned ultra-nanocapacitor; 3) the instantaneous load current has been dynamically tuned through a proportional controller in a closed-loop control scheme by simultaneously considering harvesting and discharging processes. The resulting system is described in Section II through a nonlinear state equation. The acceptable range of values of the proportional control gain guaranteeing technological constraints and asymptotic stability of the system around the equilibrium point is discussed in Section III. Then, a numerical example is presented in Section IV to clearly show the behavior of the proposed approach in conceivable scenarios. The main findings of the letter and future research activities are finally drawn in Section V.

V. Musa, G. Piro, L.A. Grieco, and G. Boggia are with the Department of Electrical and Information Engineering (DEI), Politecnico di Bari, Italy, and with Consorzio Nazionale Interuniversitario per le Telecomunicazioni (CNIT) (e-mail: {vittoria.musa, giuseppe.piro, alfredo.grieco, gennaro.boggia}@poliba.it).

TABLE I
LIST OF THE MAIN SYMBOLS USED IN THIS LETTER

Symbol	Description
T_b, T_s	Time interval needed to release a burst of molecules and symbol duration
$\eta(t)$, η_0	Duty cycle of the signal to transmit and its average value
π	Occurrence probability of bit 1
v_n, R_n, C_n	Generator voltage, resistance, and capacitance of the ultra-nanocapacitor of circuit modeling the harvesting process
h_n	Amount of harvested energy per cycle
t_n	Time duration of the harvesting cycle
$i_n(t)$, $i_l(t)$, $i_c(t)$	Generator current, load current, and current through the ultra-nanocapacitor
$p(t)$	Transmission power
k_p	Proportional gain of the controller
$V_c(t)$, $\dot{V}_c(t)$	Voltage across the ultra-nanocapacitor and its variation
E_0	Set point of the closed-loop control scheme
$E(t)$	Available energy budget at the ultra-nanocapacitor
V_∞	Equilibrium point of the closed-loop control scheme
Q_m	Minimum number of emitted molecules for bit 1
ϕ_m	Minimum amount of energy required to transmit bit 1
ξ	Conversion rate from electrical to chemical energy

II. SYSTEM MODEL

The system modeled herein considers an electrochemical nano-device supplied with a piezoelectric nanogenerator, willing to transmit information messages via diffusion-based molecular communication. The main analytical symbols used in this letter are reported in Table I.

At the physical layer, transmitter and receiver nano-devices are supposed to be synchronized. This goal can be achieved by means of one of the mechanisms already proposed in the current state of the art [2], [19], [20]. Moreover, long sequence of bits is delivered according to the On-Off Keying modulation scheme [21]. Thus, the bit 1 is encoded with the transmission of a burst of molecules, released in a very tiny time interval, T_b, while the bit 0 is encoded with the silence (no molecules are transmitted). A fixed symbol duration, lasting $T_s \gg T_b$, is also considered. The duty cycle of the transmission signal, $\eta(t)$, represents the ratio between the amount of time spent to release a burst of molecules and the symbol duration. Assuming a probability of occurrence of bit 1 equal to π, its average value is equal to $\eta_0 = \pi T_b/T_s$. The amount of energy required to generate and release a burst of molecules is assumed to be comparable with the one consumed by pure biological systems leveraging the diffusion-based molecular communication [4]. Given the distance between transmitter and receiver, the number of released molecules strictly influences the system behavior [21]. Therefore, it is possible to define the minimum number of molecules that guarantees the desired level of performance, i.e., Q_m, and the related energy consumption, ϕ_m.

Harvesting and discharging processes are shown in Fig. 1. The harvesting process uses an array of Zinc Oxide nanowires [11], [12] to generate an alternating current signal and a rectifier element to convert it into a direct current source [13], [15]. In line with [13], [15], it is modeled through an ideal voltage source, v_n, in series with a resistor, R_n. This source provides an amount of charge per cycle, h_n, every t_n seconds,

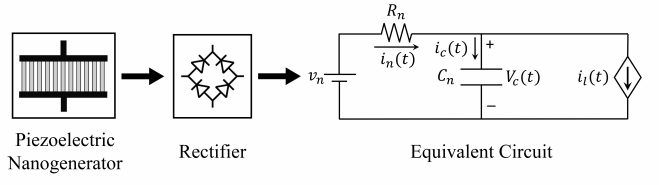

Fig. 1. Equivalent circuit of harvesting and discharging processes.

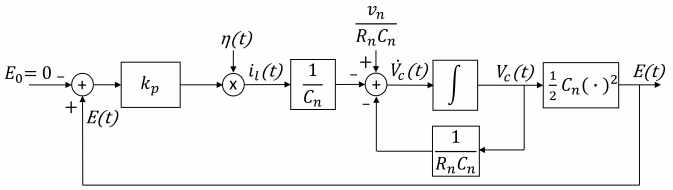

Fig. 2. The conceived closed-loop control scheme.

which already takes into account the energy loss due to the conversion between the mechanical energy and the circuit actual current. Let $i_n(t)$ be the generator current. The resulting harvested energy is stored within a ultra-nanocapacitor with capacitance C_n. In particular, $i_c(t)$ and $V_c(t)$ are the current and the voltage across the ultra-nanocapacitor, respectively. The energy budget available at the ultra-nanocapacitor feeds the transmission. Assuming a load in parallel with the ultra-nanocapacitor, the related discharging process is modeled by means of a current source with an instantaneous load current $i_l(t)$. The conversion from electrical energy to molecules includes two main processes. First, the electrical energy stored within the ultra-nanocapacitor is converted to chemical energy through an electrochemical process, which introduces a conversion rate ξ [22]. Second, the chemical energy is used to generate and release molecules into the medium [18]. Accordingly, the power transmission (i.e., the number of molecules releasable in a time unit) can be simply derived by considering the load current, $i_l(t)$, the voltage across the ultra-nanocapacitor, $V_c(t)$, and the conversion rate ξ:

$$p(t) = \xi i_l(t) V_c(t). \tag{1}$$

The methodology formulated in this letter supposes to tune the instantaneous load current $i_l(t)$ with a proportional controller in a closed-loop control scheme. The system is analytically modeled by considering the voltage across the ultra-nanocapacitor, $V_c(t)$, as the state variable. The resulting feedback control approach is depicted in Fig. 2. With the aim of ensuring a positive energy consumption during the transmission process, the control law is designed in order to obtain a positive value of $i_l(t)$. To this end, two important assumptions are introduced: the proportional gain of the controller, k_p, can only assume positive values (i.e., $k_p > 0$) and the energy budget available at the ultra-nanocapacitor, $E(t)$, is considered as the feedback variable. At the same time, in order to obtain an instantaneous load current $i_l(t)$ proportionally to the available energy budget, a null set point, i.e., $E_0 = 0$, is considered. Since $E(t) = \frac{1}{2} C_n V_c(t)^2$, the resulting closed-loop control scheme is nonlinear.

To sum up, harvesting and discharging processes lead to a variation of the state variable in the time domain, $\dot{V}_c(t)$, described through a state equation.

Theorem 1. *The state equation describing the variation of the voltage across the ultra-nanocapacitor of the considered system is:*

$$\dot{V}_c(t) = \frac{v_n}{R_n C_n} - \frac{V_c(t)}{R_n C_n} - \frac{k_p \eta(t) {V_c(t)}^2}{2}. \quad (2)$$

Proof. With reference to the circuit depicted in Fig. 1, the Kirchhoff laws state that:

$$v_n = R_n i_n(t) + V_c(t) = R_n i_c(t) + R_n i_l(t) + V_c(t). \quad (3)$$

As well known, the variation of the voltage across the ultra-nanocapacitor depends on the current through the capacitor $i_c(t)$ and its capacitance C_n, that is $\dot{V}_c(t) = i_c(t)/C_n$. Therefore, $i_c(t)$ can be written as:

$$i_c(t) = \dot{V}_c(t) C_n. \quad (4)$$

Due to the devised control approach, the load current $i_l(t)$ is proportional to the amount of available energy, $E(t)$, and the duty cycle of the signal to transmit, $\eta(t)$:

$$i_l(t) = k_p E(t) \eta(t) = \frac{k_p C_n \eta(t) {V_c(t)}^2}{2}. \quad (5)$$

Now, substituting (4) and (5) in (3), it holds:

$$v_n = R_n C_n \dot{V}_c(t) + R_n \frac{k_p C_n \eta(t) {V_c(t)}^2}{2} + V_c(t). \quad (6)$$

After a bit of algebra, it is possible to finalize the proof. □

III. Stability analysis

The stability of the nonlinear system modeled in Section II is now evaluated around the equilibrium point.

Theorem 2. *Given the nonlinear system modeled in Section II, a valid equilibrium point for the considered system is:*

$$V_\infty = \frac{-1 + \sqrt{1 + 2\eta_0 v_n k_p R_n C_n}}{\eta_0 k_p R_n C_n}. \quad (7)$$

Proof. For a continuous-time system, the equilibrium points can be found by assuming a constant input and by imposing $\dot{V}_c(t) = 0$. The constant input is set to the average duty cycle of the signal to transmit, i.e., η_0. Therefore, by posing $V_c(t) = V_\infty$ and $\eta(t) = \eta_0$ in (2), equilibrium points can be found by solving the following second-order equation:

$$\frac{k_p \eta_0}{2} {V_\infty}^2 + \frac{1}{R_n C_n} V_\infty - \frac{v_n}{R_n C_n} = 0. \quad (8)$$

This equation has two roots. The first one is $V_{\infty 1} = \frac{-1-\sqrt{1+2\eta_0 v_n k_p R_n C_n}}{\eta_0 k_p R_n C_n}$. Since $k_p > 0$, $V_{\infty 1}$ is always negative. By inverting the polarization of the voltage across the ultra-nanocapacitor, the Kirchhoff first law applied to the circuit in Fig. 1 stands that $i_l(t) = i_c(t) + i_n(t) > i_n(t)$. This means that, at the equilibrium, the load drains more current than the one generated by the harvesting process. Therefore, $V_{\infty 1}$ is not an admissible equilibrium point. Conversely, the second root, $V_{\infty 2} = \frac{-1+\sqrt{1+2\eta_0 v_n k_p R_n C_n}}{\eta_0 k_p R_n C_n}$, provides an acceptable equilibrium point. This concludes the proof. □

As initially anticipated, the control law has been designed by imposing $k_p > 0$. Nevertheless, other considerations should be done for obtaining the suitable range of values of the proportional gain k_p.

Theorem 3. *The acceptable range of values of the proportional control gain k_p is:*

$$\frac{-A - \sqrt{A^2 - B}}{D} \leq k_p \leq \frac{-A + \sqrt{A^2 - B}}{D} \quad (9)$$

where $A = v_n \xi T_s (3\phi_m R_n - {v_n}^2 \xi T_s)$, $B = 4{\phi_m}^3 \xi T_s {R_n}^3$, and $D = {\phi_m}^2 \eta_0 C_n {R_n}^3$.

Proof. The proof is achieved by considering four conditions.

First, the equilibrium point obtained by Theorem 2 must be defined in the real domain. Accordingly, the squared root and the denominator cannot assume negative and zero values, respectively, that is:

$$1 + 2\eta_0 v_n k_p R_n C_n \geq 0 \text{ and } \eta_0 k_p R_n C_n \neq 0. \quad (10)$$

Analytically, (10) is satisfied if $k_p \geq -\frac{1}{2\eta_0 v_n R_n C_n}$ and $k_p \neq 0$. Therefore, considering the initial assumption on the proportional gain (i.e., $k_p > 0$), this first condition is always verified.

Second, as highlighted in the proof of Theorem 2, the equilibrium point must assume positive values (i.e., $V_\infty > 0$). This condition is always verified when $k_p > 0$.

The third condition refers to the maximum voltage across the ultra-nanocapacitor. The equilibrium point cannot exceed the source voltage, v_n, that is $V_\infty \leq v_n$. Analytically:

$$V_\infty = \frac{-1 + \sqrt{1 + 2\eta_0 v_n k_p R_n C_n}}{\eta_0 k_p R_n C_n} \leq v_n. \quad (11)$$

The (11) is verified when $k_p > 0$. Also in this case, the initial assumption on the proportional gain of the controller (i.e., $k_p > 0$) ensures that this second condition is always satisfied.

Finally, the load current $i_l(t)$ at the equilibrium provided by the closed-loop control scheme should ensure the transmission of the minimum number of molecules that guarantees the desired level of performance: $p(t) T_s|_{V_\infty, \eta_0} \geq \phi_m$. Indeed, given (1) and (5), it holds:

$$p(t) T_s|_{V_\infty, \eta_0} = \frac{1}{2} \xi C_n \eta_0 T_s k_p {V_\infty}^3 \geq \phi_m. \quad (12)$$

Analytically, (12) is verified if $\frac{-A-\sqrt{A^2-B}}{D} \leq k_p \leq \frac{-A+\sqrt{A^2-B}}{D}$.

To sum up, considering all the analyzed conditions, the fourth constraint determines the upper and the lower bounds to the acceptable range of values of k_p, concluding the proof. □

Theorem 4. *The system having a state equation described in* (2) *is asymptotically stable around V_∞ for any $k_p > 0$.*

Proof. The state equation in (2), also reported in what follows as $\dot{V}_c(t) = f(V_c(t), \eta(t))$, refers to a nonlinear system. Nevertheless, in a small neighborhood of the equilibrium point, V_∞, the aforementioned system can be assumed to be linear.

Hence, it is possible to introduce a linearization around the equilibrium point, V_∞, by using the Taylor series:

$$\begin{aligned}\dot{V}_c(t) &= f(V_c(t),\eta(t)) \approx \\ &\approx f(V_\infty,\eta_0)+\nabla f(V_\infty,\eta_0)\cdot\begin{bmatrix}\Delta V_c(t)\\ \Delta\eta(t)\end{bmatrix},\end{aligned} \tag{13}$$

where $f(V_\infty,\eta_0)=0$ by definition, $\Delta V_c(t)=V_c(t)-V_\infty$ and $\Delta\eta(t)=\eta(t)-\eta_0$. By considering the variable $\Delta\dot{V}_c(t)$, the linearized state equation is:

$$\begin{aligned}\Delta\dot{V}_c(t) &= \left.\frac{\partial f(V_c(t),\eta(t))}{\partial V_c(t)}\right|_{V_\infty,\eta_0}\Delta V_c(t)+ \\ &+ \left.\frac{\partial f(V_c(t),\eta(t))}{\partial \eta(t)}\right|_{V_\infty,\eta_0}\Delta\eta(t) = \\ &= \left(-\frac{1}{R_nC_n}-\eta_0 V_\infty k_p\right)\Delta V_c(t)-\frac{k_p {V_\infty}^2}{2}\Delta\eta(t) = \\ &= X\Delta V_c(t)+Y\Delta\eta(t).\end{aligned} \tag{14}$$

Now, given the linearized state equation around the equilibrium point, the considered system is asymptotically stable if the coefficient that multiplies $\Delta V_c(t)$ in (14) is less than 0 [23], that is:

$$X=\left(-\frac{1}{R_nC_n}-\eta_0 V_\infty k_p\right)<0. \tag{15}$$

By substituting (7) in (15), it brings to the following inequality $-\frac{\sqrt{1+2\eta_0 v_n k_p R_n C_n}}{R_nC_n}<0$, which is always verified. Therefore, considering the initial assumption on the proportional gain (i.e., $k_p>0$), the modeled system is asymptotically stable around V_∞. □

Theorem 4 highlights that the stability analysis around the equilibrium point does not further restrict the study presented by Theorem 3. Therefore, it is possible to conclude that the acceptable range of values of the proportional gain k_p given by (9) makes the system asymptotically stable around V_∞.

IV. Numerical investigation

The following numerical example intends to show the behavior of the proposed approach in conceivable scenarios. The proposed study considers a physical symbol duration $T_s=1$ s [21]. Accordingly, T_b is set to 1 ms. Assuming a probability of occurrence of bit 1, π, equal to 0.5, the average duty cycle is set to $\eta_0=\pi\frac{T_b}{T_s}=5\cdot10^{-4}$. The time duration of the harvesting cycle is set to $t_n=1$ s. Regarding the energy harvesting mechanism, a conceivable value for the generator voltage is 0.42 V, as highlighted in [13], [24]. Furthermore, the amount of harvested charge per cycle, h_n, and the capacitance of the ultra-nanocapacitor, C_n, are directly affected by the technology used to fabricate the ultra-nanocapacitor and the size of both piezoelectric nanogenerator and ultra-nanocapacitor [13], [25], [26]. This letter considers a ultra-nanocapacitor based on onion-like carbon electrodes [13], [26] and a reasonable size for both piezoelectric nanogenerator and ultra-nanocapacitor ranging from 100 μm^2 to 1000 μm^2 [13], [25]. In the first case, $h_n=0.6$ pC and $C_n=0.9$ nF. In the second case, $h_n=6$ pC and $C_n=9$ nF. The source resistor is set to $R_n=\frac{v_n t_n}{h_n}$ [13]. The electrical energy stored within the ultra-nanocapacitor is supposed to be converted to chemical energy through the water electrolysis process, which presents a conversion rate equal to $\xi=40\%$ [22]. The chemical energy is used to generate insulin molecules through the polymerization of amino acids. According to [4], the process requires the presence of raw materials (i.e., amino acids) within the nano-device and an amount of chemical energy to bind amino acids. Thus, considering $Q_m=10^3$ and the model presented in [4], the minimum amount of energy required to transmit a burst of molecules encoding the bit 1 is set to $\phi_m=0.023$ pJ.

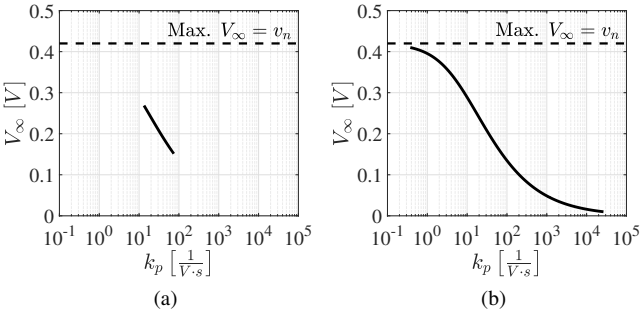

Fig. 3. Equilibrium point, V_∞, as a function of the proportional gain, k_p, when (a) $C_n=0.9$ nF and $h_n=0.6$ pC, and (b) $C_n=9$ nF and $h_n=6$ pC.

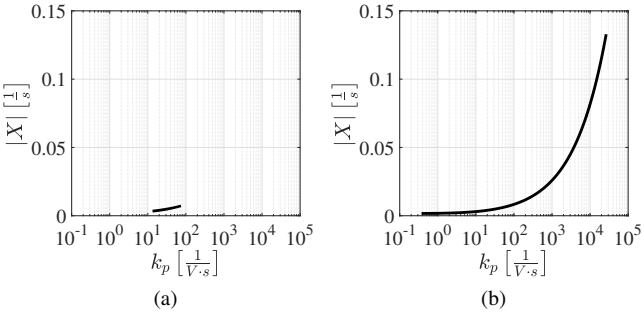

Fig. 4. Modulus of the pole of the closed-loop control scheme, $|X|$, as a function of the proportional gain, k_p, when (a) $C_n=0.9$ nF and $h_n=0.6$ pC, and (b) $C_n=9$ nF and $h_n=6$ pC.

Fig. 3 shows that the equilibrium point decreases with k_p. A higher value of k_p leads to an increment of the percentage of energy budget consumed for transmitting a single burst of molecules, while reaching lower values of the voltage across the ultra-nanocapacitor at the equilibrium point. Proposed results also demonstrate that the range of acceptable values of k_p is drastically limited by the dimension of both piezoelectric nanogenerator and ultra-nanocapacitor.

Fig. 4 illustrates the effect of k_p on the absolute value of X, as defined in (15). Specifically, X corresponds to the pole of the examined closed-loop control scheme. According to the control theory, the time response of the system decreases when $|X|$ increases. Thus, a high value of k_p is preferable to obtain a system which rapidly returns at the equilibrium state after a perturbation of the duty cycle $\eta(t)$ of the signal to transmit. This means that the dimension of both piezoelectric nano-

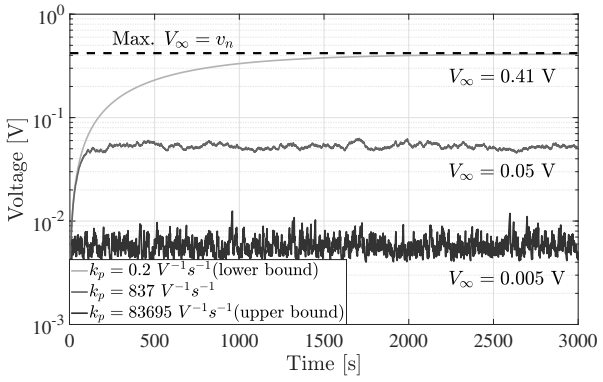

Fig. 5. Variation of the state variable, $V_c(t)$, in the time domain during the transmission of a long sequence of bits, by considering three different acceptable values of k_p, $C_n = 9$ nF, $h_n = 6$ pC, and $v_n = 0.42$ V.

generator and ultra-nanocapacitor directly affect the minimum time response of the formulated control system.

Fig. 5 depicts the variation of the state variable, $V_c(t)$, in the time domain during the transmission of a long sequence of bits, by considering three different acceptable values of k_p, $C_n = 9$ nF, $h_n = 6$ pC, and $v_n = 0.42$ V. The analysis starts assuming an initial energy budget equal to ϕ_m. It confirms that the developed system is asymptotically stable around the equilibrium point, V_∞. A higher value of k_p corresponds to a lower equilibrium point and the time required to reach the equilibrium point increases when k_p decreases.

V. Conclusion

This letter proposed a feedback control approach for an energy-harvesting and diffusion-based molecular communication system, that dynamically tunes the instantaneous load current drained by the transmitter interface through a proportional controller. After deriving the state equation of the nonlinear system, the analysis of its stability and technological constraints provided the acceptable range of values for the proportional gain. The numerical example illustrated the behavior of the formulated approach in conceivable scenarios. Future research activities will investigate how the control law affects system performance, while jointly considering other parameter settings for the proposed harvesting and discharging models, reception procedure, synchronization, and various network configurations. Moreover, the study of electrochemical processes, the definition of the type of molecules, the reaction that generates/releases them and related requirements represent a key challenge to face to move from theory to practice in this promising research field.

References

[1] I. F. Akyildiz, M. Pierobon, and S. Balasubramaniam, "Moving forward with molecular communication: from theory to human health applications [point of view]," *Proc. IEEE*, vol. 107, no. 5, pp. 858–865, 2019.

[2] N. Farsad, H. B. Yilmaz, A. Eckford, C. Chae, and W. Guo, "A comprehensive survey of recent advancements in molecular communication," *IEEE Commun. Surveys Tuts.*, vol. 18, no. 3, pp. 1887–1919, 2016.

[3] M. B. Dissanayake, Y. Deng, A. Nallanathan, M. Elkashlan, and U. Mitra, "Interference mitigation in large-scale multiuser molecular communication," *IEEE Trans. Commun.*, 2019.

[4] M. Ş. Kuran, H. B. Yilmaz, T. Tugcu, and B. Özerman, "Energy model for communication via diffusion in nanonetworks," *Nano Commun. Netw.*, vol. 1, no. 2, pp. 86–95, 2010.

[5] Y. Deng, W. Guo, A. Noel, A. Nallanathan, and M. Elkashlan, "Enabling energy efficient molecular communication via molecule energy transfer," *IEEE Commun. Lett.*, vol. 21, no. 2, pp. 254–257, Feb 2017.

[6] M. Kuscu, E. Dinc, B. Bilgin, H. Ramezani, and O. Akan, "Transmitter and receiver architectures for molecular communications: A survey on physical design with modulation, coding, and detection techniques," *Proc. IEEE*, pp. 1–40, 2019.

[7] S. Sudevalayam and P. Kulkarni, "Energy harvesting sensor nodes: Survey and implications," *IEEE Commun. Surveys Tuts.*, vol. 13, no. 3, pp. 443–461, 2010.

[8] M.-L. Ku, W. Li, Y. Chen, and K. R. Liu, "Advances in energy harvesting communications: Past, present, and future challenges," *IEEE Commun. Surveys Tuts.*, vol. 18, no. 2, pp. 1384–1412, 2015.

[9] S. Mohrehkesh, M. C. Weigle, and S. K. Das, "Energy harvesting in electromagnetic nanonetworks," *Computer*, vol. 50, no. 2, pp. 59–67, Feb 2017.

[10] S. Chandrasekaran, C. Bowen, J. Roscow, Y. Zhang, D. K. Dang, E. J. Kim, R. Misra, L. Deng, J. S. Chung, and S. H. Hur, "Micro-scale to nano-scale generators for energy harvesting: Self powered piezoelectric, triboelectric and hybrid devices," *Physics Reports*, 2018.

[11] L. Wei, Q.-X. Liu, B. Zhu, W.-J. Liu, S.-J. Ding, H.-L. Lu, A. Jiang, and D. W. Zhang, "Low-cost and high-productivity three-dimensional nanocapacitors based on stand-up zno nanowires for energy storage," *Nanoscale research letters*, vol. 11, no. 1, p. 213, 2016.

[12] Z. L. Wang and J. Song, "Piezoelectric nanogenerators based on zinc oxide nanowire arrays," *Science*, vol. 312, no. 5771, pp. 242–246, 2006.

[13] J. M. Jornet and I. F. Akyildiz, "Joint energy harvesting and communication analysis for perpetual wireless nanosensor networks in the terahertz band," *IEEE Trans. Nanotechnol.*, vol. 11, no. 3, pp. 570–580, 2012.

[14] M. Donohoe, B. Jennings, J. M. Jornet, and S. Balasubramaniam, "Nanodevice arrays for peripheral nerve fascicle activation using ultrasound energy-harvesting," *IEEE Trans. Nanotechnol.*, vol. 16, no. 6, pp. 919–930, 2017.

[15] S. A. Wirdatmadja, M. T. Barros, Y. Koucheryavy, J. M. Jornet, and S. Balasubramaniam, "Wireless optogenetic nanonetworks for brain stimulation: Device model and charging protocols," *IEEE Trans. Nanobiosci.*, vol. 16, no. 8, pp. 859–872, Dec 2017.

[16] J.-T. Huang and C.-H. Lee, "On capacity bounds of two-way diffusion channel with molecule harvesting," in *Proc. IEEE ICC*, 2017, pp. 1–6.

[17] H. G. Bafghi, A. Gohari, M. Mirmohseni, G. Aminian, and M. Nasiri-Kenari, "Diffusion based molecular communication with limited molecule production rate," *IEEE Trans. Mol. Biol. Multi-Scale Commun.*, 2019.

[18] W. Guo, Y. Deng, H. B. Yilmaz, N. Farsad, M. Elkashlan, A. Eckford, A. Nallanathan, and C. Chae, "Smiet: Simultaneous molecular information and energy transfer," *IEEE Wireless Commun.*, vol. 25, no. 1, pp. 106–113, 2018.

[19] M. Mukherjee, H. B. Yilmaz, B. B. Bhowmik, J. Lloret, and Y. Lv, "Synchronization for diffusion-based molecular communication systems via faster molecules," in *Proc. IEEE ICC*, 2019, pp. 1–5.

[20] H. ShahMohammadian, G. G. Messier, and S. Magierowski, "Blind synchronization in diffusion-based molecular communication channels," *IEEE Commun. Lett.*, vol. 17, no. 11, pp. 2156–2159, November 2013.

[21] M. Kuscu and O. B. Akan, "Maximum likelihood detection with ligand receptors for diffusion-based molecular communications in internet of bio-nano things," *IEEE Trans. Nanobiosci.*, vol. 17, no. 1, pp. 44–54, Jan 2018.

[22] S. P. Badwal, S. S. Giddey, C. Munnings, A. I. Bhatt, and A. F. Hollenkamp, "Emerging electrochemical energy conversion and storage technologies," *Frontiers in chemistry*, vol. 2, p. 79, 2014.

[23] H. Khalil, *Nonlinear Systems: Pearson New International Edition*, ser. Always Learning. Pearson Education Limited, 2013.

[24] S. Xu, B. J. Hansen, and Z. L. Wang, "Piezoelectric-nanowire-enabled power source for driving wireless microelectronics," *Nature communications*, vol. 1, p. 93, 2010.

[25] S. Canovas-Carrasco, A.-J. Garcia-Sanchez, and J. Garcia-Haro, "On the nature of energy-feasible wireless nanosensor networks," *Sensors*, vol. 18, no. 5, p. 1356, 2018.

[26] D. Pech, M. Brunet, H. Durou, P. Huang, V. Mochalin, Y. Gogotsi, P.-L. Taberna, and P. Simon, "Ultrahigh-power micrometre-sized supercapacitors based on onion-like carbon," *Nature nanotechnol.*, vol. 5, no. 9, p. 651, 2010.